Am J Transl Res 2018;10(4):1053-1070
www.ajtr.org /ISSN:1943-8141/AJTR0067395

Original Article

Adipose-derived mesenchymal stem cell-derived exosomes alleviate overwhelming systemic inflammatory reaction and organ damage and improve outcome in rat sepsis syndrome

Chia-Lo Chang[1], Pei-Hsun Sung[2,9], Kuan-Hung Chen[5], Pei-Lin Shao[6], Chih-Chao Yang[3], Ben-Chung Cheng[3], Kun-Chen Lin[5], Chih-Hung Chen[4], Han-Tan Chai[2,9], Hsueh-Wen Chang[7], Hon-Kan Yip[2,6,8,9,10*], Hong-Hwa Chen[1*]

[1]Division of Colorectal Surgery, Department of Surgery, Kaohsiung Chang Gung Memorial Hospital and Chang Gung University College of Medicine, Kaohsiung 83301, Taiwan, China; Divisions of [2]Cardiology, [3]Nephrology, [4]General Medicine, Department of Internal Medicine, Kaohsiung Chang Gung Memorial Hospital and Chang Gung University College of Medicine, Kaohsiung 83301, Taiwan, China; [5]Department of Anesthesiology, Kaohsiung Chang Gung Memorial Hospital and Chang Gung University College of Medicine, Kaohsiung 83301, Taiwan, China; [6]Department of Nursing, Asia University, Taichung 41354, Taiwan, China; [7]Department of Biological Sciences, National Sun Yat-sen University, Kaohsiung 80424, Taiwan, China; [8]Institute for Translational Research in Biomedicine, [9]Center for Shockwave Medicine and Tissue Engineering, Kaohsiung Chang Gung Memorial Hospital, Kaohsiung 83301, Taiwan, China; [10]Department of Medical Research, China Medical University Hospital, China Medical University, Taichung 40402, Taiwan, China. [*]Equal contributors.

Received October 17, 2017; Accepted December 14, 2017; Epub April 15, 2018; Published April 30, 2018

Abstract: This study tested the hypothesis that healthy adipose-derived mesenchymal stem cell (ADMSC)-derived exosomes ($HMSC^{EXO}$) and apoptotic (A) (induced by 12 h hypoxia/12 h starvation)-ADMSC-derived exosomes ($AMSC^{EXO}$) were comparably effective at alleviating sepsis syndrome [SS; induced by cecal-ligation and puncture (CLP)]-induced systemic inflammation and reduced organ damage and unfavorable outcomes in rats. SD rats were divided into sham control (SC), SS only, SS + $HMSC^{EXO}$ (100 μg intravenous administration 3 h after CLP), and $AMSC^{EXO}$. By day 5 after CLP procedure, the mortality rate was significantly higher in SS than in SC and $HMSC^{EXO}$ (all $P < 0.01$), but it showed no significant different between SC and $HMSC^{EXO}$, between $AMSC^{EXO}$ and $HMSC^{EXO}$ or between SS and $AMSC^{EXO}$ ($P > 0.05$). The levels of inflammatory mediators in circulation ($CD11^{b/c}$/Ly6G/MIF), bronchioalveolar lavage ($CD11^{b/c}$/Ly6G) and abdominal ascites ($CD11^{b/c}$/CD14/Ly6G/MIF) were highest in SS, lowest in SC and significantly higher in $AMSC^{EXO}$ than in $HMSC^{EXO}$ (all $P < 0.001$). The circulating/splenic levels of immune cells (CD34+/CD4+/CD3+/CD8+) were expressed in an identical pattern whereas the T-reg+ cells exhibited an opposite pattern of inflammation among the groups (all $P < 0.001$). The protein expressions of inflammation (MMP-9/MIF/TNF-α/NF-κB/IL-1β) and oxidative stress (NOX-1/NOX-2/oxidized protein), and cellular expressions (CD14+/CD68+) in lung/kidney parenchyma exhibited an identical pattern of inflammatory mediators (all $P < 0.001$). The kidney/lung injury scores displayed an identical pattern of inflammatory mediators among the groups (all $P < 0.001$). In conclusion, $HMSC^{EXO}$ might be superior to $AMSC^{EXO}$ for improving survival and suppressing the inflammatory reactions in rats after SS.

Keywords: Sepsis syndrome, adipose-derived mesenchymal stem cell-derived exosomes, inflammation

Introduction

Sepsis syndrome (SS), i.e., systemic inflammatory response associated with infection, is a common public health issue and a major health problem worldwide, and results in a heavy economic burden through health care costs in developed countries [1-3]. Despite advanced pharmaceutical therapies, continuous evolution of new antibiotics, hygiene education programs and upgrades in guidelines for health education and prevention of infection, SS remains one of major leading causes of death in hospitalized patients for any disease worldwide [4-7]. Especially, in ICUs, SS causes unacceptable high mortality, ranging from 35% from

sepsis to over 60% from septic shock [1-9]. Clearly, there is an urgent need for innovative and efficacious therapies for SS.

The incidence of SS and its prognosis are clear [1-3, 8]; however, its underlying mechanisms remain heavily debated [8, 10-12]. Overwhelming inflammation is proposed to play a crucial role in the patient/host response to septic challenge [8, 12]. This hyper-inflammatory response involves the innate immune system [8, 10-13], neutrophil and macrophage accumulation [12], cytokine secretion [10, 14], recruitment of T and B cells [12, 15] and the formation of antibodies [16] in an attempt to eliminate causative pathogens but this process also causes bystander attack on the major organs/tissues, leading to anergy of host-defense mechanisms, rapid organ failure and potential decline to death [17].

Exosomes, one kind of micro-vesicles derived from a variety of cells, are membrane fragments with a size of around 60-120 nm [18-20]. Additionally, exosomes contain distinct subsets of microRNAs depending upon the cell type from which they are secreted [21]. Furthermore, a growing body of experimental data has revealed that the mesenchymal stem cell (MSC)-derived exosomes which are involved in (1) angiogenesis, (2) immunomodulation, (3) anti-inflammation and (4) the paracrine effect improve organ function following injury in preclinical studies [21-26]. Interestingly, much evidence has demonstrated that stem cells, especially adipose-derived mesenchymal stem cells (ADMSCs), possess intrinsic capacity for immunomodulation [27, 28]; therefore, attenuating inflammation and immune responses [27-29]. We previously showed that apoptotic-ADMSC therapy is more effective than healthy-ADMSC therapy at inhibiting SS-induced inflammation and oxidative stress, as well as mortality in rats [30]. Several reports [18-30] have raised the hypothesis that exosomes derived from apoptotic ADMSCs should be comparable to exosomes derived from healthy ADMSCs for inhibiting inflammatory reactions and improving unfavorable outcomes in SS.

Materials and methods

Animals and ethics statement

All animal experimental protocols and procedures were approved by the Institute of Animal Care and Use Committee at Kaohsiung Chang Gung Memorial Hospital and performed in accordance with the Guide for the Care and Use of Laboratory Animals [The Eighth Edition of the Guide for the Care and Use of Laboratory Animals (NRC 2011)].

Animals were housed in an Association for Assessment and Accreditation of Laboratory Animal Care International (AAALAC)-approved animal facility in our hospital with controlled temperature and light cycles (24°C and 12/12 light cycle).

Procedure for SS induction by cecal ligation and puncture (CLP), sham operated control (SC) and measurement of tail systolic blood pressure (SBP)

Pathogen-free, adult male Sprague-Dawley (SD) rats weighing 320-350 g (Charles River Technology, BioLASCO, Taiwan) were utilized in the present study.

Rats were anesthetized with inhalational 2.0% isoflurane and placed supine on a warming pad at 37°C with the abdomen shaved. Under sterile conditions, the abdominal skin and muscle were opened and the cecum exposed in all groups. In the SP control animals, the abdomen was then closed and the animal was allowed to recover from anesthesia. In the experimental CLP groups, the cecum was prolene suture ligated over its distal portion (i.e., distal ligation) and the cecum distal to the ligature was punctured twice with an 18# needle to allow the cecal contents to be expressed intraperitoneally, as previously described [30]. The wound was closed and the animal was allowed to recover from anesthesia.

The tail SBP was measured (Kent Scientific Corporation, Model no: CODA, U.S.A.) based on our recent investigation [30] by a technician who was blinded to the treatment protocols at 28 h (for surviving animals) after CLP or sham procedure. In brief, the blood pressure was measured at this interval as the majority of animals were weakest at a time interval within 18-30 h. The tail cuff approach to BP measurement was conducted as follows: Initially the rats were warmed in a box at 37°C for 20 minutes before being placed in a restraining apparatus which was also kept at 37°C. The tail was inserted through the cuff which contained a photoelectric pulse detector through which the

SBP were recorded when the first oscillation appeared during the gradual reduction of cuff pressure. Mean BP was determined from the cuff pressure when the amplitude of the oscillation reached its maximum. The SBP was consecutively and continuously measured 30 times for each rat. Data of SBP were recorded for the first 10 times; and recordings made when the animals were agitated were discarded. Finally, reliable SBP data were averaged for each rat and expressed as mean ± SD.

Animal groups and treatment strategy

The adult male SD rats (n = 71) were categorized into SC (n = 16), SS (n = 19), healthy (H) ADMSC-derived exosomes ($HMSC^{EXO}$) (n = 18) (i.e., 100 μg intravenous administration 3 h after CLP) and apoptotic (A)-ADMSC-derived exosomes ($AMSC^{EXO}$) (n = 18) (treatment route and dosage was identical $HMSC^{EXO}$). The exosome dosage was as described in our previous report [22].

Isolation of ADMSCs

For prepared allogenic ADMSCs, an additional 20 SD rats were utilized in the current study. Adipose tissue surrounding the epididymis was dissected, excised and prepared based on our recent reports [31, 32]. Then, 300 μL of sterile saline was added to every 0.5 g of adipose tissue to prevent dehydration. The tissue was carefully cut into < 1 mm^3 size pieces using a pair of sharp, sterile surgical scissors. Sterile saline (37°C) was added to the homogenized adipose tissue in a ratio of 3:1 (saline: adipose tissue), followed by the addition of stock collagenase solution to a final concentration of 0.5 units/mL. The centrifuge tubes with the contents were placed and secured on a Thermaline shaker and incubated with constant agitation for 60 minutes at 37°C. After 40-45 minutes of incubation, the contents were triturated with a 25-mL pipette for 3 minutes. The isolated cells were put back into the rocker for incubation. The contents of the flask were transferred to 50 mL tubes after digestion, followed by centrifugation at 600 g for 5 minutes at room temperature. The fatty layer and saline supernatant from the tube were discarded gently in one smooth motion or removed using vacuum suction. The cell pellet thus obtained was resuspended in 40 mL saline and then centrifuged again at 600 g for 5 minutes at room temperature. After being resuspended again in 5-mL saline, the cell suspension was filtered through a 100 μm filter into a 50-mL conical tube to which 2 mL of saline was added to rinse the remaining cells through the filter. The flow-through was pipetted into a new 50-mL conical tube through a 40-μm filter. The tubes were centrifuged for a third time at 600 g for 5 minutes at room temperature. The cells were resuspended in saline. An aliquot of cell suspension was then removed for cell culture in Dulbecco's modified Eagle's medium (DMEM)-low glucose medium containing 10% FBS for 14 days. Approximately 2.0-3.0×10^6 ADMSCs were obtained from each rat.

Preparation, isolation and dosage of exosomes

The preparation, isolation and dosage of ADMSC-derived exosomes were based on our recent report [24]. The exosomes were isolated from the culture medium of ADMSCs and were pooled for protein separation and characterization, as well as western blot analysis. The proteins in Dulbecco's modified Eagle medium (DMEM) (Gibco) supplemented with 10% serum before and after cell culture were separated by sodium dodecyl sulfate-polyacrylamide gel electrophoresis (SDS-PAGE). The exosomes in DMEM were purified and the proteins in different exosome fractions (1 μg, 2 μg, 10 μg, and 50 μg) were also separated by SDS-PAGE. The gel was stained with Coomassie blue for analysis. The following primary antibodies were used: mouse monoclonal anti-CD63 (Santa Cruz Biotechnology), rabbit polyclonal anti-tumor susceptibility gene-101 (TSG101) (Abcam) and anti-β-catenin (Abcam).

Definition of apoptotic ADMSCs and preparation of $AMSC^{EXO}$

Serum deprivation of cells in vitro for induction of apoptosis was performed according to previous [33] and our recent [30] studies with some modifications. Hence, ADMSC were first cultured in normal culture medium followed by 12 hours of hypoxia (1% oxygen) and 12 hours of serum-free cell culture. The percentages of viable and apoptotic cells were determined by flow cytometry using double staining of annexin V and propidium iodide (PI). This is a simple and popular method for the identification of apoptotic cells (i.e., early [annexin V+/PI-] and late [annexin V+/PI+] phases of apoptosis). The purpose of serum deprivation and hypoxia of the

ADMSCs was to create a stress for the ADMSCs, i.e., preconditioning. Therefore, we defined this preconditioning of ADMSCs as $AMSC^{EXO}$. Therefore, for preparation of ($AMSC^{EXO}$), (i.e., allogenic exosomes), the ADMSC were cultured under hypoxic conditions for 12 h and starvation (i.e., serum deprivation in cell culturing) for 12 h, followed by exosome collection.

Analysis of circulating level of TNF-α

Blood samples were drawn from rats in each group and stored at -80°C until analyses of tumor necrosis factor (TNF)-α was performed in batches at the end of the experiment. Serum TNF-α concentration was assessed in duplicate with a commercially available ELISA kit (R& D Systems, Minneapolis, MN). Intra-individual variability in TNF-α level was assessed in each group with the mean intra-assay coefficient of variance < 1.8%.

Isolation of splenic mononuclear cells for assessment of immune cells

Mononuclear cells in the spleen were obtained by homogenization of the spleen using a Tenbroeck tissue grinder followed by passage through a 0.4-mm-pore-size cell strainer to obtain a single cell suspension. These cells were then suspended in RPMI and separated by Ficoll-paque Plus (GE Healthcare) for identification of immune cells.

Flow cytometric quantifications of inflammatory cells in circulation bronchoalveolar lavage (BAL) circulation and ascites, and helper, cytotoxic, and regulatory (Tregs) T cells in circulation and in the spleen

Flow cytometric analysis was performed to identify and characterize immune cells and inflammatory cell surface markers. The procedure and protocol of flow cytometric analysis for immune cells was based on our recent report [30]. Briefly, peripheral blood mononuclear cells and splenocytes (1.0×10^6 cells for each population) were triple-stained with FITC-anti-CD3 (BioLegend), PE-anti-CD8a (BD Bioscience), and PE-Cy™5 anti-CD4 (BD bioscience). To identify CD4+CD25+Foxp3+ Tregs, peripheral blood mononuclear cells and splenocytes were triple-stained with Alexa Fluor 488-anti-CD25 (BioLegend), PE-anti-Foxp3 (BioLegend), and PE-Cy5 anti-CD4 (BD Bioscience) using the Foxp3 Fix/Perm buffer set according to the manufacturer's protocol. The numbers of CD3+CD4+ helper T cells, CD3+CD8+ cytotoxic T cells, and CD4+CD25+Foxp3+ Tregs were analyzed using flow cytometry (FC500, Beckman Coulter).

Kidney injury scores at day 5 after SS induction procedure

Histopathology scoring was assessed in a blinded fashion as we have previously described [29]. Briefly, the kidney specimens from all animals were fixed in 10% buffered formalin, embedded in paraffin, sectioned at 5 μm and stained with hematoxylin and eosin (H&E) for light microscopy. The scoring system reflects the grading of tubular necrosis, loss of brush border, cast formation, and tubular dilatation in 10 randomly chosen, non-overlapping fields (200×) as follows: 0 (none), 1 (≤10%), 2 (11-25%), 3 (26-45%), 4 (46-75%), and 5 (≥76%) [29].

Histological measurement of lung injury and criteria for lung injury score

The lung specimens were sectioned at 5 μm for light microscopy for each animal. H&E staining was performed to estimate the number of alveolar sacs in a blinded fashion as we previously reported [28, 34]. Three lung sections from each rat were analyzed and three randomly selected high-power fields (HPFs; 100×) were examined in each section. The mean number per HPF for each animal was then determined by summation of all numbers divided by 9. The extent of the crowded area, which was defined as the region of thickened septa in lung parenchyma associated with partial or complete collapse of alveoli on H&E-stained sections, was also measured in a blinded fashion. The following scoring system [28, 34] was adopted: 0 = no detectable crowded area; 1 = < 15% of crowded area; 2 = 15-25% of crowded area; 3 = 25-50% of crowded area; 4 = 50-75% of crowded area; 5= > 75-100% of crowded area/HPF.

Immunohistochemical (IHC) and immunofluorescent (IF) staining

The procedure and protocol for IHC and IF staining have previously been reported in detail [22, 31, 35]. For IHC and IF staining, rehydrated paraffin sections were first treated with 3% H_2O_2 for 30 minutes and incubated with Immuno-

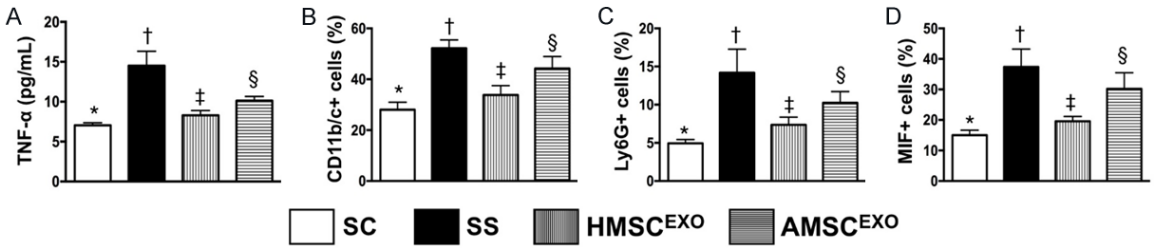

Figure 1. ELISA measurement and flow cytometric analysis for determining circulating inflammatory levels at 24 h and 72 h after SS induction. A: Circulating level of tumor necrosis factor (TNF)-α at 24 h after SS induction, * vs. other groups with different symbols (†, ‡, §), $P < 0.001$. B: Circulating level of $CD11^{b/c+}$ cells, * vs. other groups with different symbols (†, ‡, §), $P < 0.001$. C: Circulating level of Ly6G+ cells, * vs. other groups with different symbols (†, ‡, §), $P < 0.001$. D: Circulating level of macrophage migration inhibitor factor (MIF)+ cells, * vs. other groups with different symbols (†, ‡, §), $P < 0.001$. All statistical analyses were performed by one-way ANOVA, followed by Bonferroni multiple comparison post hoc test (n = 6 for each group). Symbols (*, †, ‡, §) indicate significance at the 0.05 level. SC = sham control; SS = sepsis syndrome; $AMSC^{EXO}$ = apoptotic adipose-derived mesenchymal stem cell-derived exosomes; $HMSC^{EXO}$ = healthy adipose-derived mesenchymal stem cell-derived exosomes.

Block reagent (BioSB, Santa Barbara, CA, USA) for 30 minutes at room temperature. Sections were then incubated with primary antibodies specifically against CD14 (1:50, Santa Cruz), CD68 (1:100, Abcam), and γ-H2AX (1:1000, Abcam) while sections incubated with irrelevant antibodies served as controls. Three kidney sections from each rat were analyzed. For quantification, three randomly selected HPFs (200× for IHC; 400× for IF) were analyzed in each section. The mean number of positively-stained cells per HPF for each animal was then determined by summation of all numbers divided by 9.

Western blot analysis

The procedure and protocol for Western blot analysis have been described in our previous reports [22, 31, 35]. Briefly, equal amounts (50 μg) of protein extract were loaded and separated by SDS-PAGE using acrylamide gradients. After electrophoresis, the separated proteins were transferred electrophoretically to a polyvinylidene difluoride (PVDF) membrane (Amersham Biosciences, Amersham, UK). Non-specific sites were blocked by incubation of the membrane in blocking buffer [5% nonfat dry milk in T-TBS (TBS containing 0.05% Tween 20)] overnight. The membranes were incubated with the indicated primary antibodies [matrix metalloproteinase (MMP)-9 (1:3000, Abcam, Cambridge, MA, USA), tumor necrosis factor (TNF)-α (1:1000, Cell Signaling, Danvers, MA, USA), nuclear factor (NF)-κB (1:600, Abcam, Cambridge, MA, USA), NADPH oxidase (NOX)-1 (1:1500, Sigma, St. Louis, Mo, USA), NOX-2 (1:750, Sigma, St. Louis, Mo, USA), interleukin (IL)-1β (1:1000, Cell Signaling, Danvers, MA, USA), macrophage migratory inhibitor factor (MIF) (1:2000, Abcam, Cambridge, MA, USA) and actin (1:10000, Chemicon, Billerica, MA, USA)] for 1 hour at room temperature. Horseradish peroxidase-conjugated anti-rabbit immunoglobulin IgG (1:2000, Cell Signaling, Danvers, MA, USA) was used as a secondary antibody for one-hour incubation at room temperature. The washing procedure was repeated eight times within one hour. Immunoreactive bands were visualized by enhanced chemiluminescence (ECL; Amersham Biosciences, Amersham, UK) and exposed to Biomax L film (Kodak, Rochester, NY, USA). For quantification, ECL signals were digitized using Labwork software (UVP, Waltham, MA, USA).

Assessment of oxidative stress

The procedure and protocol for assessing the protein expression of oxidative stress have been detailed in our previous reports [22, 31, 35]. The Oxyblot Oxidized Protein Detection Kit was purchased from Chemicon, Billerica, MA, USA (S7150). DNPH derivatization was carried out on 6 μg of protein for 15 minutes according to the manufacturer's instructions. One-dimensional electrophoresis was carried out on 12% SDS/polyacrylamide gel after DNPH derivatization. Proteins were transferred to nitrocellulose membranes which were then incubated in the primary antibody solution (anti-DNP 1:150) for 2 hours, followed by incubation in secondary antibody solution (1:300)

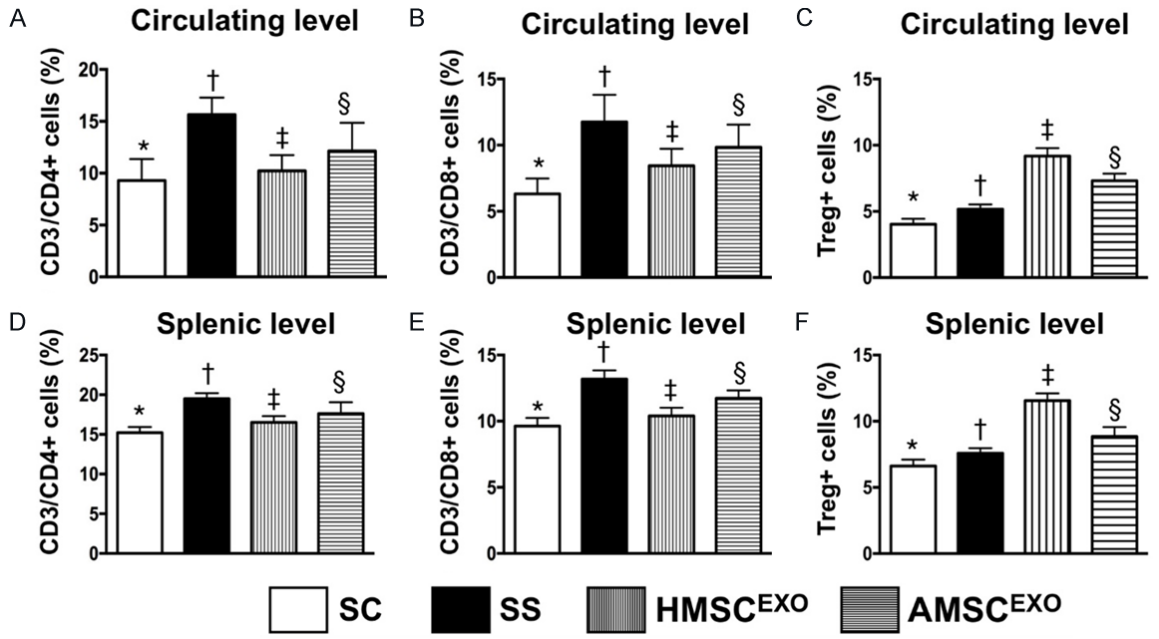

Figure 2. Flow cytometric analysis for determining circulating and splenic levels of immune cells at day 5 after SS induction. A: Circulating number of CD3/CD4+ cells, * vs. other groups with different symbols (†, ‡, §), $P < 0.001$. B: Circulating number of CD3/CD8+ cells, * vs. other groups with different symbols (†, ‡, §), $P < 0.001$. C: Circulating number of Treg+ cells, * vs. other groups with different symbols (†, ‡, §), $P < 0.001$. D: Splenic level of CD3/CD4+ cells, * vs. other groups with different symbols (†, ‡, §), $P < 0.001$. E: Splenic level of CD3/CD8+ cells, * vs. other groups with different symbols (†, ‡, §), $P < 0.001$. F: Splenic level of regulatory T (Treg)+ cells, * vs. other groups with different symbols (†, ‡, §), $P < 0.001$. All statistical analyses were performed by one-way ANOVA, followed by Bonferroni multiple comparison post hoc test (n = 6 for each group). Symbols (*, †, ‡, §) indicate significance at the 0.05 level. SC = sham control; SS = sepsis syndrome; $AMSC^{EXO}$ = apoptotic adipose-derived mesenchymal stem cell-derived exosomes; $HMSC^{EXO}$ = healthy adipose-derived mesenchymal stem cell-derived exosomes.

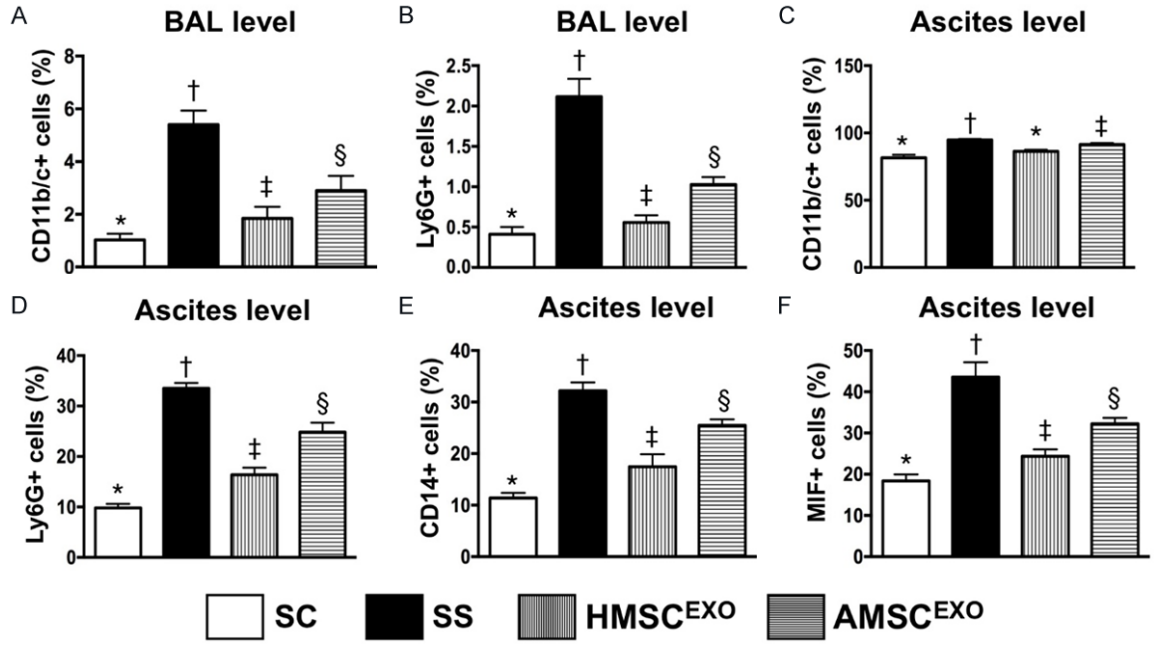

Figure 3. Flow cytometric analysis for bronchioalveolar lavage (BAL) and levels of inflammatory biomarkers in ascites at day 5 after SS induction. A: BAL level $CD11^{b/c+}$ cells, * vs. other groups with different symbols (†, ‡, §), $P < 0.001$. B: BAL level Ly6G+ cells, * vs. other groups with different symbols (†, ‡, §), $P < 0.001$. C: Level of $CD11^{b/c+}$ cells in ascites, * vs. other groups with different symbols (†, ‡, §), $P < 0.01$. D: Level of Ly6G+ cells in ascites, * vs.

other groups with different symbols (†, ‡, §), P < 0.0001. E: Level of CD14+ cells in ascites, * vs. other groups with different symbols (†, ‡, §), P < 0.0001. F: Level of macrophage migration inhibitory factor (MIF)+ cells in ascites, * vs. other groups with different symbols (†, ‡, §), P < 0.0001. All statistical analyses were performed by one-way ANOVA, followed by Bonferroni multiple comparison post hoc test (n = 6 for each group). Symbols (*, †, ‡, §) indicate significance at the 0.05 level. SC = sham control; SS = sepsis syndrome; $AMSC^{EXO}$ = apoptotic adipose-derived mesenchymal stem cell-derived exosomes; $HMSC^{EXO}$ = healthy adipose-derived mesenchymal stem cell-derived exosomes.

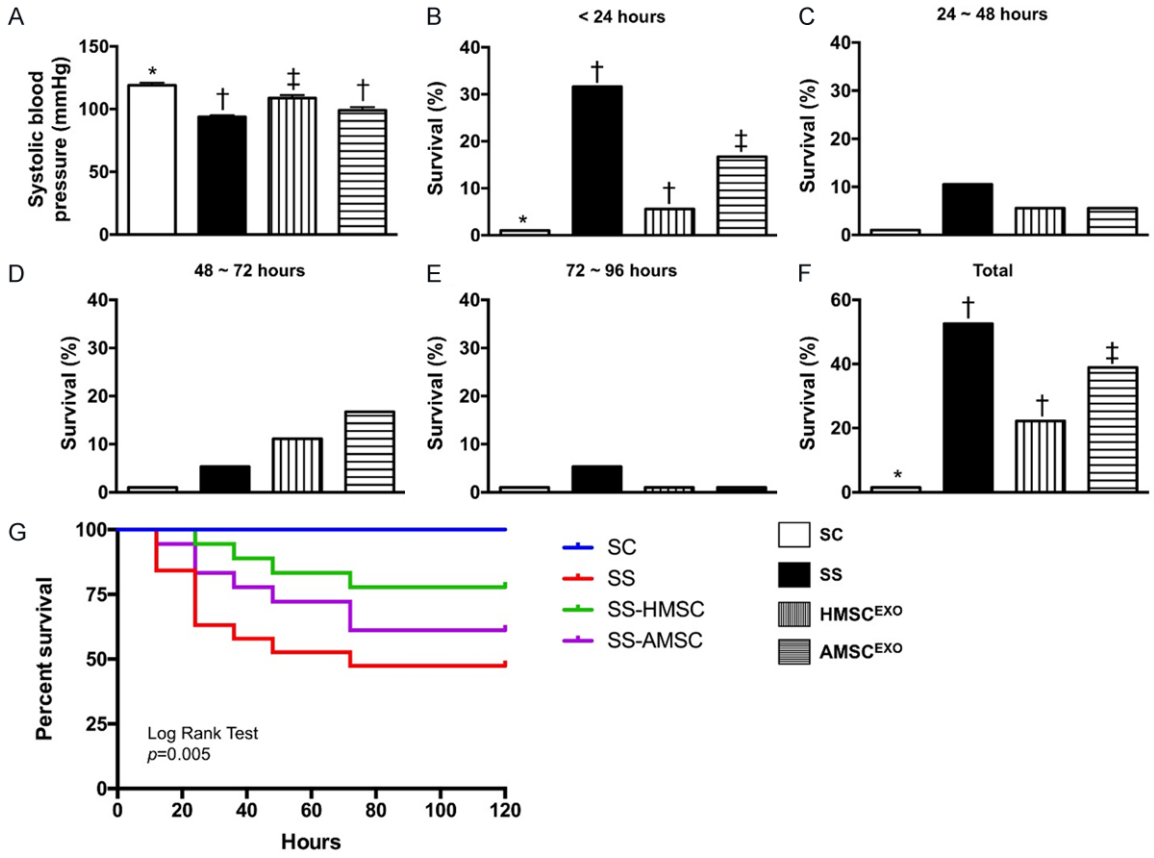

Figure 4. Blood pressure at 28 h and 5-day survival rate among the four groups of the animals. (A) The systolic blood pressure by 28 days after SS induction, * vs. other groups with different symbols (†, ‡), P < 0.0001. All statistical analyses were performed by one-way ANOVA, followed by Bonferroni multiple comparison post hoc test. Symbols (*, †, ‡) indicate significance at the 0.05 level. (B-F) Showing the time points of survival rate after SS induction. For (A) analytical results, * vs. other groups with different symbols (†, ‡), p = 0.035. (F) The survival rate of four groups by rate Pairwise comparisons (without Bonferroni's correction), * vs. †, P = 0.005. Symbols (*, †, ‡) indicate significance at the 0.05 level. (G) Kaplan Meier survival cure. By log Rank test, P = 0.005. SC = sham control; SS = sepsis syndrome; $AMSC^{EXO}$ = apoptotic adipose-derived mesenchymal stem cell-derived exosomes; $HMSC^{EXO}$ = healthy adipose-derived mesenchymal stem cell-derived exosomes.

for 1 hour at room temperature. The washing procedure was repeated eight times within 40 minutes. Immunoreactive bands were visualized by enhanced chemiluminescence (ECL; Amersham Biosciences, Amersham, UK) which was then exposed to Biomax L film (Kodak, Rochester, NY, USA). For quantification, ECL signals were digitized using Labwork software (UVP, Waltham, MA, USA). For Oxyblot protein analysis, a standard control was loaded on each gel.

Statistical analysis

Quantitative data are expressed as means ± SD. Statistical analysis was adequately performed by ANOVA followed by Bonferroni multiple-comparison post hoc test. Statistical analysis was performed using SPSS statistical software for Windows version 22 (SPSS for Windows, version 22; SPSS, IL, U.S.A.). A value of $P < 0.05$ was considered as statistically significant.

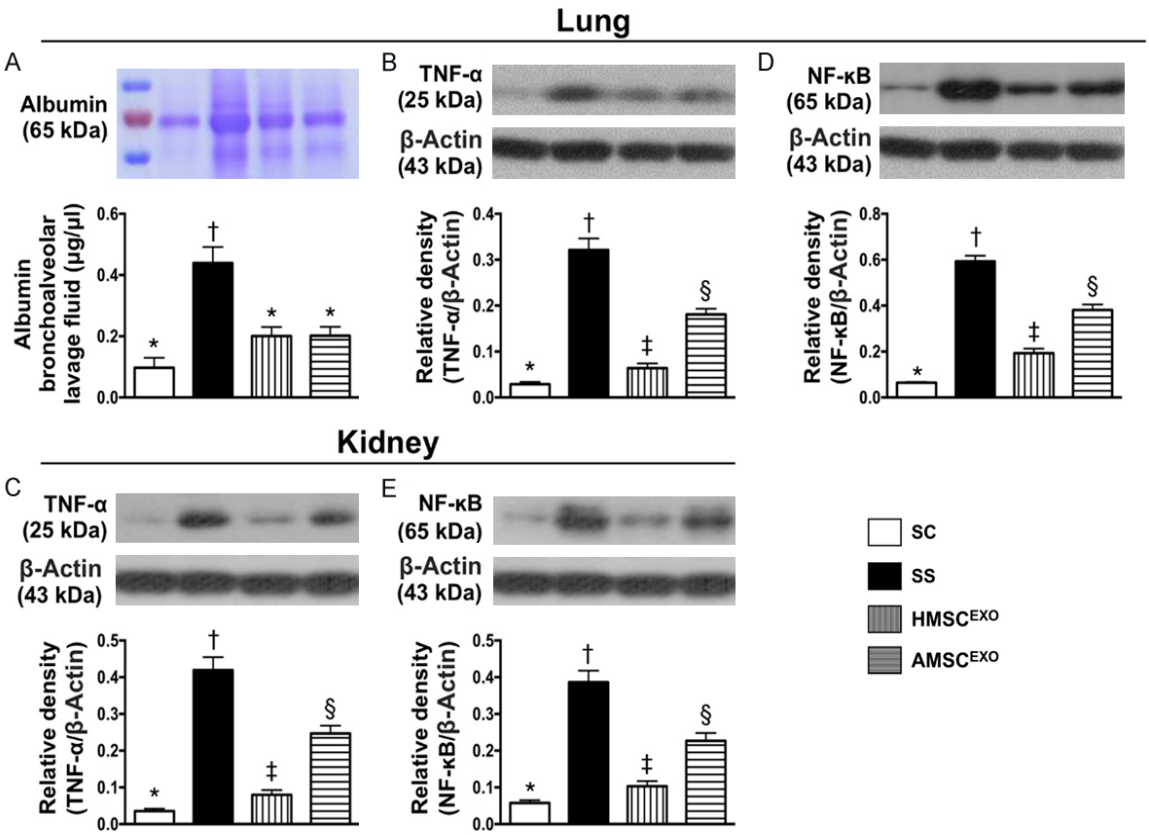

Figure 5. Albumin level of bronchoalveolar lavage (BAL) and protein expressions of inflammatory biomarkers in lung and kidney at day 5 after SS induction. A: Albumin concentrations of BAL fluid. * vs. other groups with different symbols (*, †, ‡), $P < 0.0001$. M.W. = molecular weight. B: Protein expression of tumor necrosis factor (TNF)-α at lung parenchyma, * vs. other groups with different symbols (†, ‡, §), $P < 0.0001$. C: Protein expression of TNF-α at kidney parenchyma, * vs. other groups with different symbols (†, ‡, §), $P < 0.0001$. D: Protein expression of nuclear factor (NF)-κB at lung, * vs. other groups with different symbols (†, ‡, §), $P < 0.0001$. E: Protein expression of NF-κB at kidney, * vs. other groups with different symbols (†, ‡, §), $P < 0.0001$. All statistical analyses were performed by one-way ANOVA, followed by Bonferroni multiple comparison post hoc test (n = 6 for each group). Symbols (*, †, ‡, §) indicate significance at the 0.05 level. SC = sham control; SS = sepsis syndrome; $AMSC^{EXO}$ = apoptotic adipose-derived mesenchymal stem cell-derived exosomes; $HMSC^{EXO}$ = healthy adipose-derived mesenchymal stem cell-derived exosomes.

Results

*ELISA assessment and flow cytometric analysis for determining circulating inflammatory levels at 24 h and 72 h after SS induction (**Figure 1**)*

The ELISA assessment at 24 h showed that the circulating level of TNF-α, an indication of acute innate inflammatory reaction, was highest in SS, lowest in SC and significantly lower in SS-$HMSC^{EXO}$ than in SS-$AMSC^{EXO}$. Additionally, the flow cytometric analysis demonstrated that the circulating levels of $CD11^{b/c+}$, Ly6G+ and MIF+ cells, three indices of inflammation, exhibited an identical pattern of TNF-α among the four groups.

*Flow cytometric analysis for identification of circulating and splenic levels of immune cells at day 5 after SS induction (**Figure 2**)*

The flow cytometric results showed that circulating and splenic levels of adaptive immune cells (CD3/CD4+, CD3/CD8+) were highest in SS, lowest in SC and significantly lower in SS-$HMSC^{EXO}$ than in SS-$AMSC^{EXO}$. On the other hand, circulating level of T-reg+ cells, another adaptive immune cell, displayed an opposite pattern of CD3/CD4+ cells among the four groups.

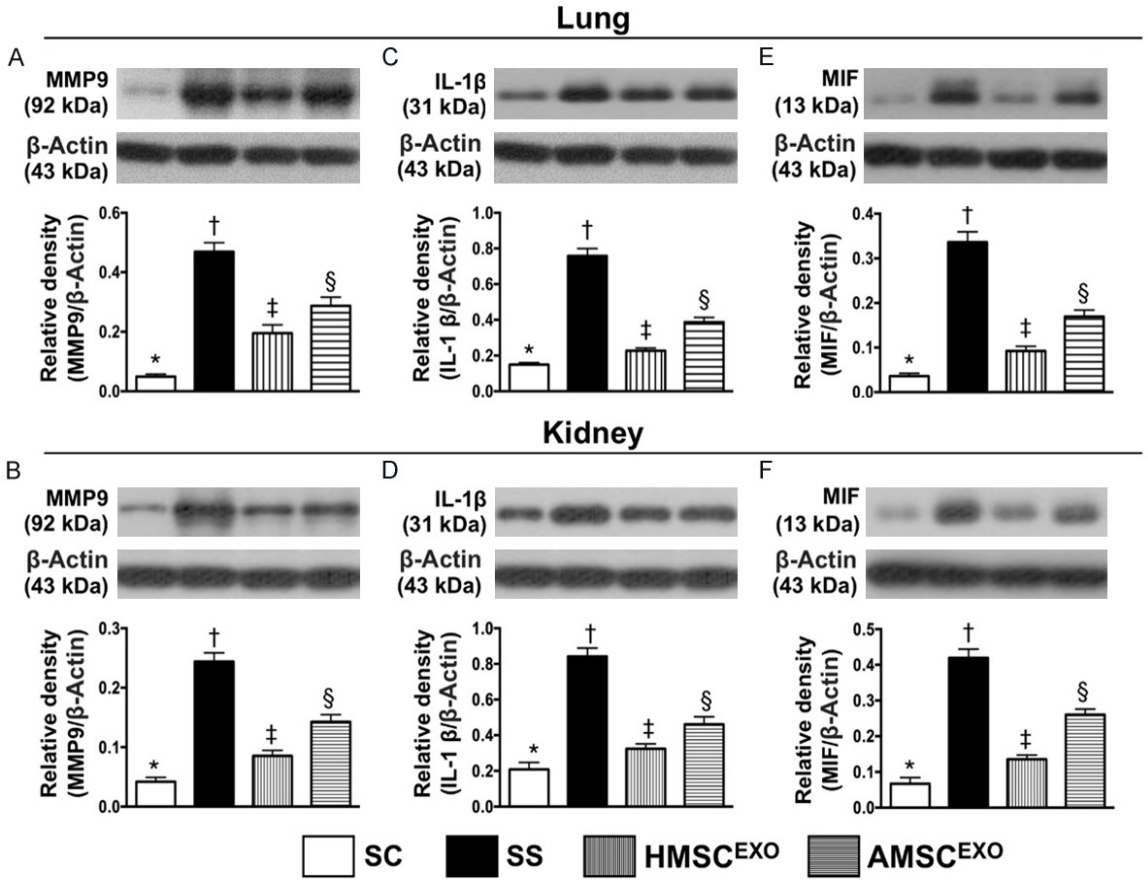

Figure 6. Protein expressions of proinflammatory cytokines in lung and kidney organs at day 5 after SS induction. A: Protein expression of matrix metalloproteinase (MMP)-9 in lung parenchyma, * vs. other groups with different symbols (†, ‡, §), P < 0.0001. B: Protein expression of MMP-9 in kidney parenchyma, * vs. other groups with different symbols (†, ‡, §), P < 0.0001. C: Protein expression of interleukin (IL)-1β lung parenchyma, * vs. other groups with different symbols (†, ‡, §), P < 0.0001. D: Protein expression of IL-1β in kidney parenchyma, * vs. other groups with different symbols (†, ‡, §), P < 0.0001. E: Protein expression of macrophage migration inhibitory factor (MIF) in lung parenchyma, * vs. other groups with different symbols (†, ‡, §), P<0.0001. F: Protein expression of MIF in kidney parenchyma, * vs. other groups with different symbols (†, ‡, §), P < 0.0001. * vs. other groups with different symbols (†, ‡, §), P < 0.0001. All statistical analyses were performed by one-way ANOVA, followed by Bonferroni multiple comparison post hoc test (n = 6 for each group). Symbols (*, †, ‡, §) indicate significance at the 0.05 level. SC = sham control; SS = sepsis syndrome; $AMSC^{EXO}$ = apoptotic adipose-derived mesenchymal stem cell-derived exosomes; $HMSC^{EXO}$ = healthy adipose-derived mesenchymal stem cell-derived exosomes.

*Flow cytometric measurement of bronchioalveolar lavage (BAL) and ascites of inflammatory biomarkers at day 5 after SS induction (**Figure 3**)*

Flow cytometric assessment showed that the BAL levels of $CD11^{b/c+}$ and Ly6G+ cells, two inflammatory mediators, were highest in SS, lowest in SC, and significantly lower in SS-$HMSC^{EXO}$ than in SS-$AMSC^{EXO}$. Additionally, this measurement showed that the ascites levels of $CD11^{b/c+}$, Ly6G+, CD14+, and MIF+ cells, four inflammatory biomarkers, exhibited an identical pattern to that of $CD11^{b/c+}$ cells in BAL among the four groups.

*Blood pressure at 28 h and 5-day survival rate among the four groups of animals (**Figure 4**)*

By 28 h after SS induction, the systolic blood pressure (SBP) was significantly higher in SC than in other groups, significantly higher SS-$HMSC^{EXO}$ than in SS and SS-$AMSC^{EXO}$, but it only showed tendency of significantly higher in SS-$AMSC^{EXO}$ than in SS. Additionally, 5-day survival rate exhibited an identical pattern of SBP among the four groups.

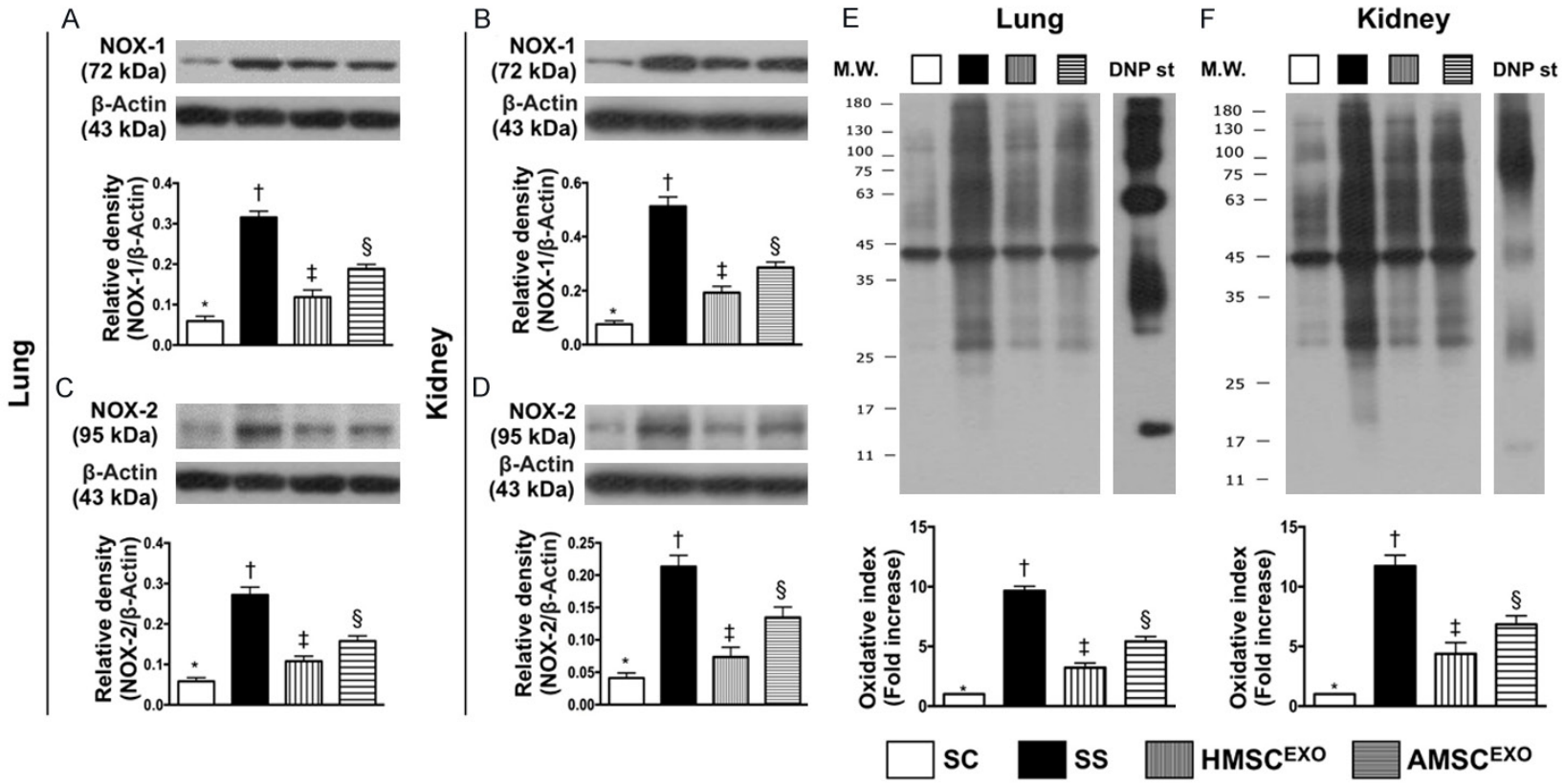

Figure 7. Protein expressions of oxidative stress biomarkers in lung and kidney organs at day 5 after SS induction. A: Protein expression of NOX-1 in lung parenchyma, * vs. other groups with different symbols (†, ‡, §), $P < 0.0001$. B: Protein expression of NOX-1 in kidney parenchyma, * vs. other groups with different symbols (†, ‡, §), $P < 0.0001$. C: Protein expression of NOX-2 in lung parenchyma, * vs. other groups with different symbols (†, ‡, §), $P < 0.0001$. D: Protein expression of NOX-2 in kidney parenchyma, * vs. other groups with different symbols (†, ‡, §), $P < 0.0001$. E: Oxidized protein expression in lung parenchyma, * vs. other groups with different symbols (†, ‡, §), $P < 0.0001$. (Note: left and right lanes shown on the upper panel represent protein molecular weight marker and control oxidized molecular protein standard, respectively). M.W. = molecular weight; DNP = 1-3 dinitrophenylhydrazone. F: Oxidized protein expression in lung parenchyma, * vs. other groups with different symbols (†, ‡, §), $P < 0.0001$. (Note: left and right lanes shown on the upper panel represent protein molecular weight marker and control oxidized molecular protein standard, respectively). M.W. = molecular weight; DNP = 1-3 dinitrophenylhydrazone. All statistical analyses were performed by one-way ANOVA, followed by Bonferroni multiple comparison post hoc test (n = 6 for each group). Symbols (*, †, ‡, §) indicate significance at the 0.05 level. SC = sham control; SS = sepsis syndrome; $AMSC^{EXO}$ = apoptotic adipose-derived mesenchymal stem cell-derived exosomes; $HMSC^{EXO}$ = healthy adipose-derived mesenchymal stem cell-derived exosomes.

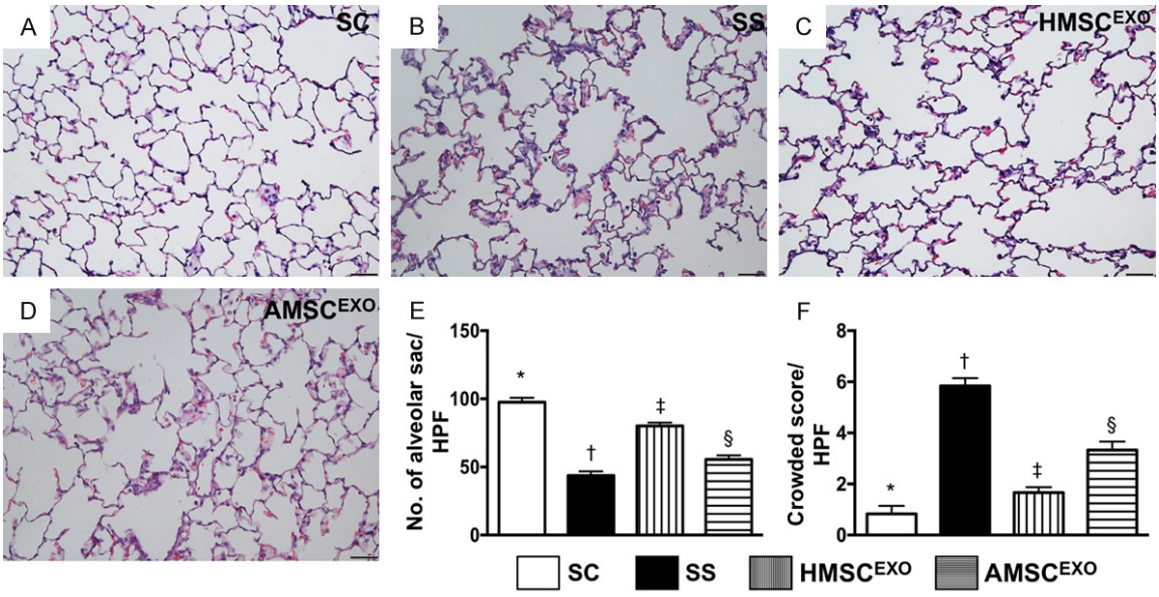

Figure 8. Histopathological findings in lung parenchyma by day 5 after SS induction. A-D: Histopathological findings (i.e., H&E staining) of lung parenchyma under microscopy (200×) among the four groups. E: The number of alveolar sacs among four groups. * vs. other groups with different symbols (†, ‡, §), $P < 0.0001$. F: Crowded scores of lung parenchyma. * vs. other groups with different symbols (†, ‡, §), $P < 0.0001$. The scale bars in right lower corner represent 50 μm. All statistical analyses were performed by one-way ANOVA, followed by Bonferroni multiple comparison post hoc test (n = 6 for each group). Symbols (*, †, ‡, §) indicate significance at the 0.05 level. SC = sham control; SS = sepsis syndrome; $AMSC^{EXO}$ = apoptotic adipose-derived mesenchymal stem cell-derived exosomes; $HMSC^{EXO}$ = healthy adipose-derived mesenchymal stem cell-derived exosomes.

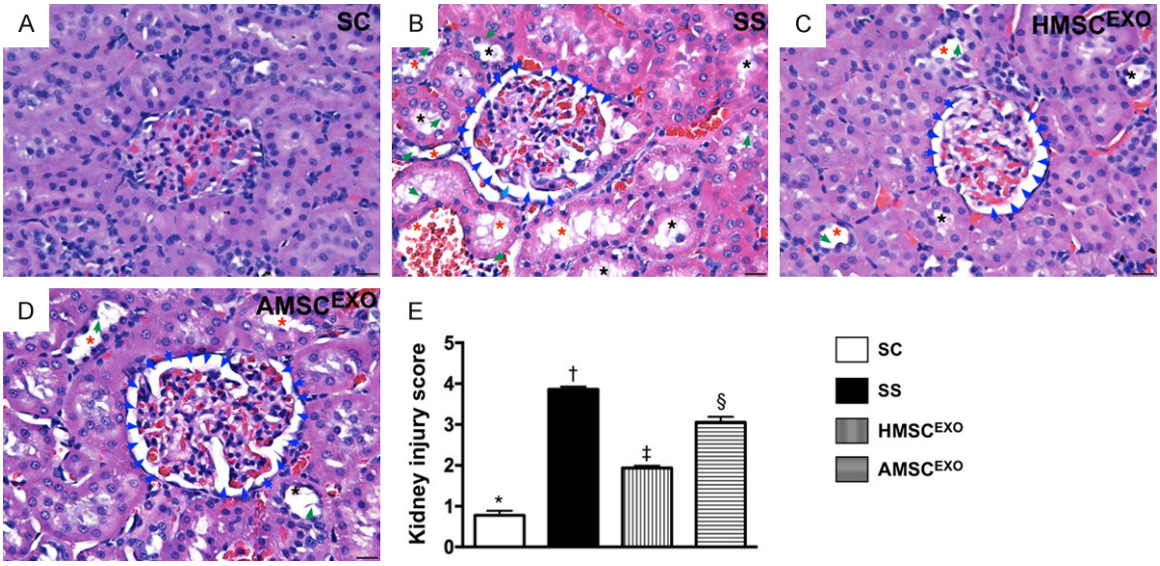

Figure 9. Histopathological findings in kidney parenchyma at day 5 after SS induction. A-D: Light microscopic findings of H&E stain (400×) demonstrating significantly higher degree of loss of brush border in renal tubules (yellow arrows), tubular necrosis (green arrows), tubular dilatation (red asterisk) protein cast formation (black asterisk), and dilatation of Bowman's capsule (blue arrows) in CKD and CKD-SS group than in other groups. E: * vs. other groups with different symbols (†, ‡, §), $P < 0.0001$. Scale bars in right lower corner represent 20 μm. All statistical analyses were performed by one-way ANOVA, followed by Bonferroni multiple comparison post hoc test (n = 6 for each group). Symbols (*, †, ‡, §) indicate significance at the 0.05 level. SC = sham control; SS = sepsis syndrome; $AMSC^{EXO}$ = apoptotic adipose-derived mesenchymal stem cell-derived exosomes; $HMSC^{EXO}$ = healthy adipose-derived mesenchymal stem cell-derived exosomes.

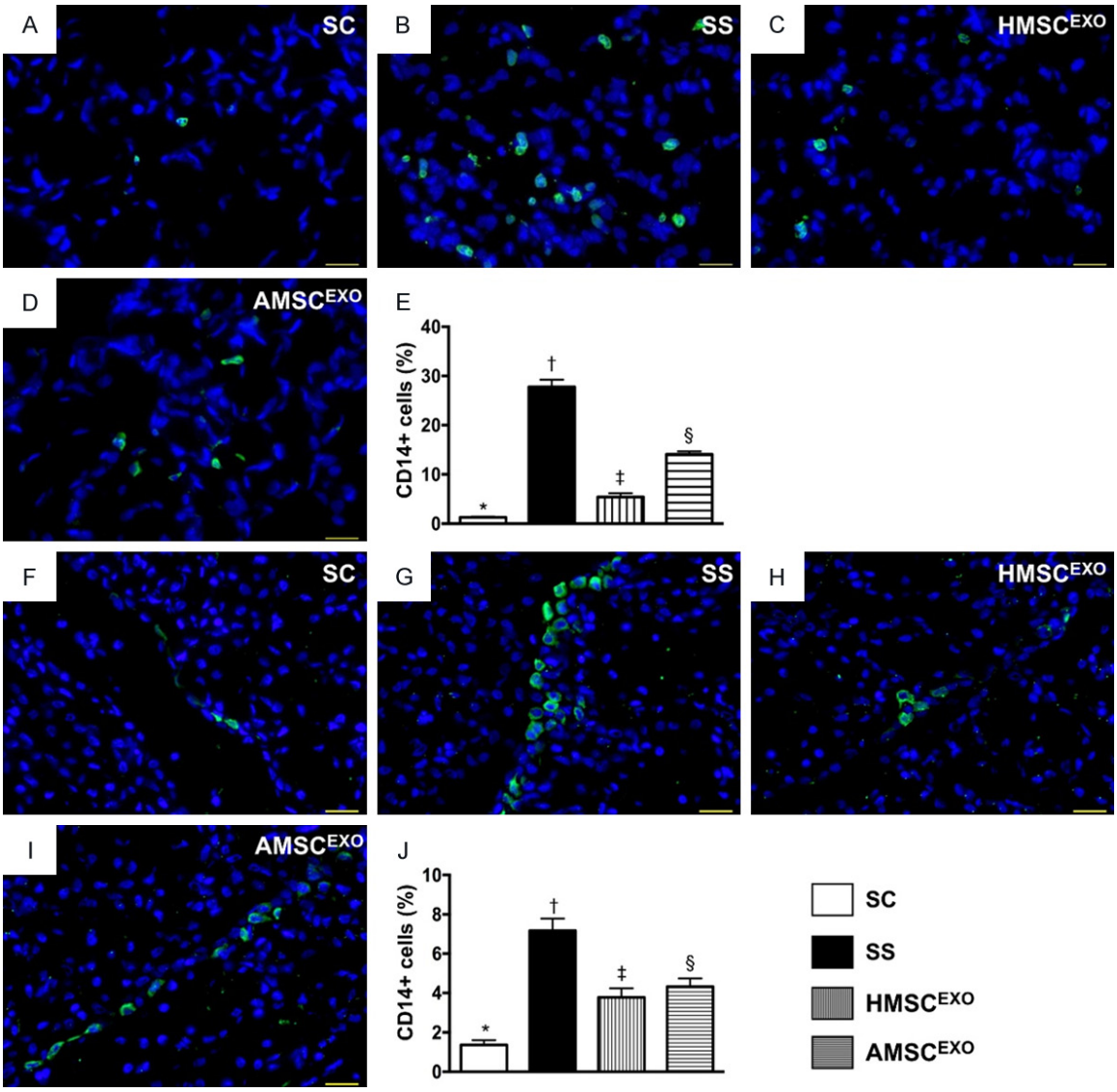

Figure 10. CD14+ infiltrations in lung and kidney organs at day 5 after SS induction. A-D: Immunofluorescent (IF) microscopic findings (400) for identification of CD14+ cells (green color) in lung parenchyma. E: Analytical results of number of CD14+ cells, * vs. other groups with different symbols (†, ‡, §), $P < 0.0001$. F-I: IF microscopic finding (400×) for identification of CD14+ cells (green color) in kidney parenchyma. J: Analytical results of number of CD14+ cells, * vs. other groups with different symbols (†, ‡, §), $P < 0.0001$. Scale bars in right lower corner represent 20 μm. All statistical analyses were performed by one-way ANOVA, followed by Bonferroni multiple comparison post hoc test (n = 6 for each group). Symbols (*, †, ‡, §) indicate significance at the 0.05 level. SC = sham control; SS = sepsis syndrome; $AMSC^{EXO}$ = apoptotic adipose-derived mesenchymal stem cell-derived exosomes; $HMSC^{EXO}$ = healthy adipose-derived mesenchymal stem cell-derived exosomes.

*Albumin level of BAL and protein expressions of inflammatory biomarkers in lung and kidney parenchyma at day 5 after SS induction (**Figures 5** and **6**)*

The albumin level of BAL, an indicator of SS-induced exudate leakage in lung parenchyma, was highest in SS, lowest in SC, significantly higher in SS-$AMSC^{EXO}$ than in SS-$HMSC^{EXO}$ (**Figure 5**). Additionally, the protein expression of TNF-α and NF-κB in lung and kidney organs, two indicators of inflammatory mediators, exhibited an identical pattern of albumin level of BAL among the four groups (**Figure 5**).

The protein expressions of MMP-9, IL-1β, and MIF in lung and kidney parenchyma, another three inflammatory biomarkers, displayed an identical pattern to albumin level of BAL among the four groups (**Figure 6**).

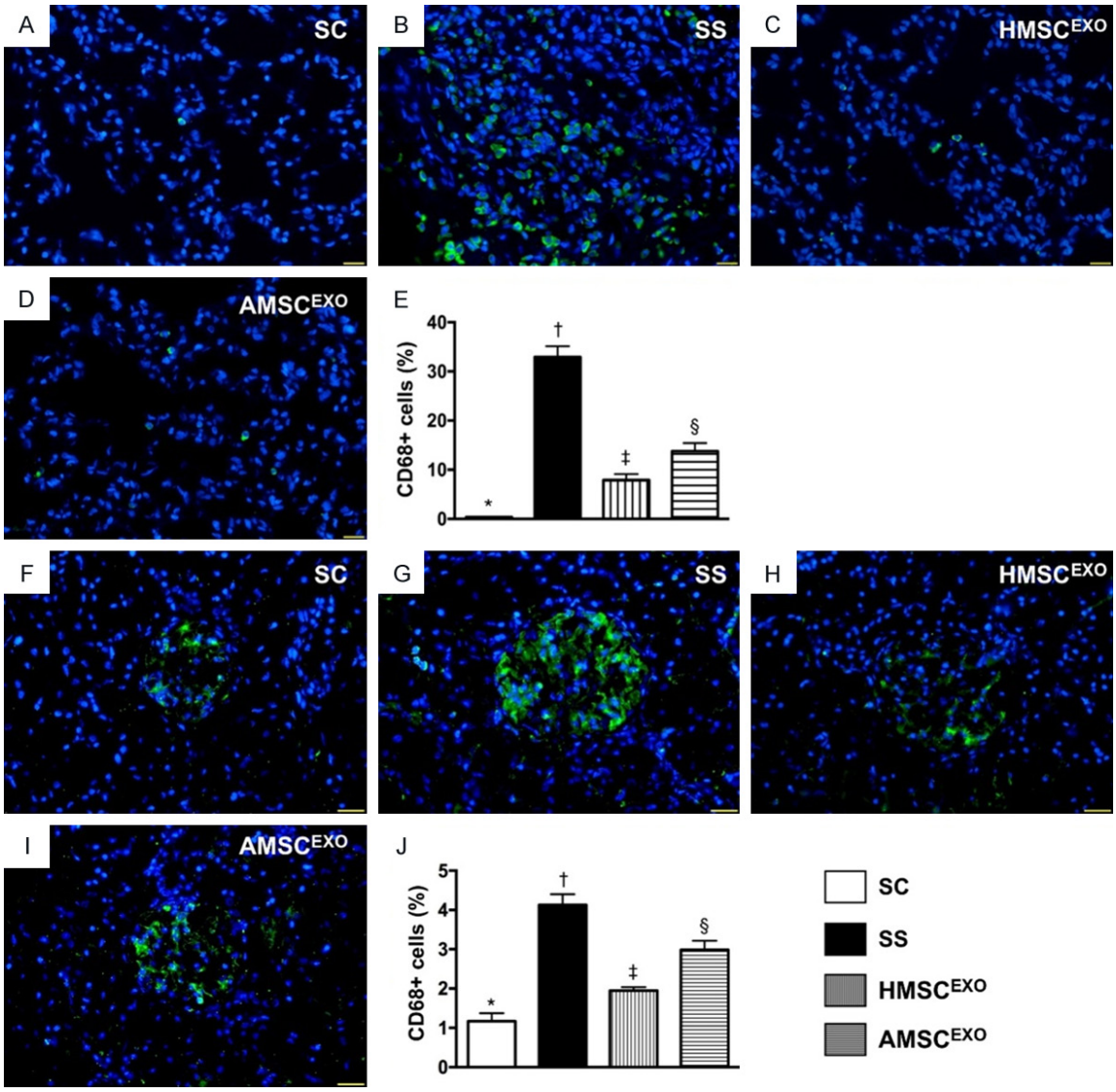

Figure 11. CD68+ infiltrations in lung and kidney organ at day 5 after SS induction. A-D: Immunofluorescence (IF) microscopy findings (400) for identification of CD68+ cells (green color) in lung parenchyma. E: Analytical results of number of CD68+ cells, * vs. other groups with different symbols (†, ‡, §), $P < 0.0001$. F-I: IF microscopic finding (400×) for identification of CD68+ cells (green color) in kidney parenchyma. J: Analytical results of number of CD68+ cells, * vs. other groups with different symbols (†, ‡, §), $P < 0.0001$. Scale bars in right lower corner represent 20 μm. All statistical analyses were performed by one-way ANOVA, followed by Bonferroni multiple comparison post hoc test (n = 6 for each group). Symbols (*, †, ‡, §) indicate significance at the 0.05 level. SC = sham control; SS = sepsis syndrome; $AMSC^{EXO}$ = apoptotic adipose-derived mesenchymal stem cell-derived exosomes; $HMSC^{EXO}$ = healthy adipose-derived mesenchymal stem cell-derived exosomes.

*Protein expressions of oxidative stress biomarkers in lung and kidney organs at day 5 after SS induction (**Figure 7**)*

The protein expressions of NOX-1, NOX-2 and oxidized protein in lung and kidney organs, three indices of oxidative stress, were highest in SS, lowest in SC and significantly higher in SS-$AMSC^{EXO}$ than in SS-$HMSC^{EXO}$.

*Histopathological findings in lung and kidney parenchyma at day 5 after SS induction (**Figures 8** and **9**)*

Histopathological analyses with H&E tissue staining demonstrated that the number of alveolar sacs was lowest in SS, highest in SC, and significantly lower in SS-$AMSC^{EXO}$ than in SS-$HMSC^{EXO}$ (**Figure 8**). Conversely, lung paren-

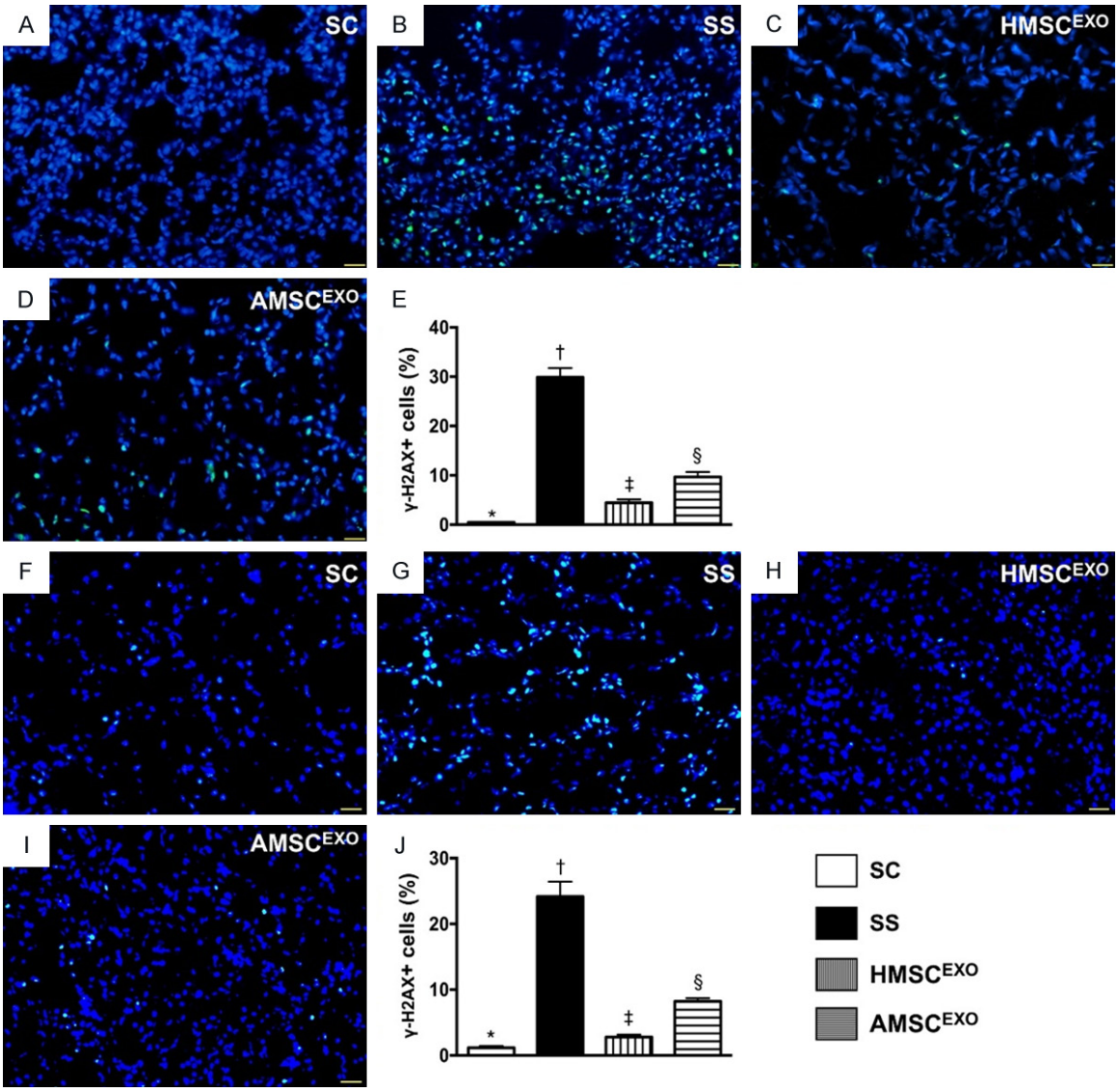

Figure 12. Cellular expression of DNA-damage marker in lung and kidney organs at day 5 after SS induction. A-D: Immunofluorescence (IF) microscopic findings (400) for identification of γ-H2AX+ cells (green color) in lung parenchyma. E: Analytical results of number of γ-H2AX+ cells, * vs. other groups with different symbols (†, ‡, §), $P < 0.0001$. F-I: IF microscopic findings (400×) for identification of γ-H2AX+ cells (green color) in kidney parenchyma. J: Analytical results of number of γ-H2AX+ cells, * vs. other groups with different symbols (†, ‡, §), $P < 0.0001$. Scale bars in right lower corner represent 20 μm. All statistical analyses were performed by one-way ANOVA, followed by Bonferroni multiple comparison post hoc test (n = 6 for each group). Symbols (*, †, ‡, §) indicate significance at the 0.05 level. SC = sham control; SS = sepsis syndrome; $AMSC^{EXO}$ = apoptotic adipose-derived mesenchymal stem cell-derived exosomes; $HMSC^{EXO}$ = healthy adipose-derived mesenchymal stem cell-derived exosomes.

chymal crowding showed a reverse pattern compared to that of the number of alveolar sacs among the four groups.

Additionally, the microscopy findings also demonstrated that the kidney injury score exhibited an identical pattern to lung parenchymal crowding among the four groups (**Figure 9**).

*Inflammatory cell infiltrations in lung and kidney parenchyma at day 5 after SS induction (**Figures 10** and **11**)*

The IF microscopic findings showed that the CD14+ cells in lung and kidney parenchyma, an indicator of inflammation, was highest in SS, lowest in SC and significantly higher in SS-

AMSC^{EXO} than in SS-HMSC^{EXO} (**Figure 10**). Additionally, the IF microscopic findings demonstrated that the CD68+ cells in lung and kidney parenchyma, another indicator of inflammation, displayed an identical pattern of CD14+ cells among the four groups (**Figure 11**).

*Cellular expression of DNA-damage marker in lung and kidney parenchyma at day 5 after SS induction (**Figure 12**)*

The IF microscopy findings showed that the cellular expression of γ-H2AX, a DNA-damage biomarker, was highest in SS, lowest in SC and significantly higher in SS-AMSC^{EXO} than in SS-HMSC^{EXO}.

Discussion

This study investigated the impact of ADMS-derived exosome therapy on reducing organ damage and improving outcome in SS in rat yielded several implications. First, our results showed that SS not only induced local but also elicited systemic inflammatory (i.e., innate) and immune (i.e., adaptive) reactions. Second, an association between increasing inflammatory/immune mediators and enhancing lung/kidney organ damage was clearly identified in the current study. Third, a comparable effect for inhibiting inflammatory/immune reactions, alleviating lung/kidney organ injury and reducing the mortality in rats after SS was clearly identified in the present study.

Our previous studies [30, 36] showed that an experimental model of CLP-induced SS usually causes 50% to 60% mortality within 3-5 days in rodents. An essential finding in the present study was that the 5-day mortality was 52.6% in SS animals. Accordingly, our finding, in addition to being comparable with the findings of our previous studies [30, 36], once again proves that our animal model of SS is consistent. Our studies have recently demonstrated that both autologous apoptotic/healthy ADMSC [30, 36] and even xenogenic MSC therapy significantly improved mortality in rodents after SS. The most important finding in the present study was that as compared with SS animals without treatment, the mortality rate was remarkably reduced in SS animals after receiving healthy ADMSC derived- or apoptotic ADMSC-derived exosome treatment. Accordingly, our findings, in addition to supporting our hypothesis, extended the findings of our recent reports [30, 36]. Intriguingly, our recent studies [22, 24, 35] have shown that ADMSC-derived exosomes improved the outcomes in ischemia-related organ damage settings. In this way, our findings strengthened the findings of our recent studies [22, 24, 35].

Overwhelming inflammatory response involving the innate and adoptive immune system has been well recognized [8, 10-13]. In addition, the inflammatory cell infiltration in the damaged organs [12], cytokine production [10, 14] and recruitment of T and B cells (i.e., immune cells) [12, 15, 16] have also been clearly established by previous studies. A principal finding in the present study was that both systemic and localized inflammatory reactions were substantially increased in SS animals. Additionally, the pro-inflammatory cytokines and immune cells were markedly upregulated in SS animals. Our findings, therefore, were consistent with the findings of previous studies [8, 10-16]. Importantly, these molecular-cellular perturbations were significantly alleviated in those SS animals after receiving apoptotic ADMSC-derived or healthy ADMSC-derived exosomes, suggesting that apoptotic ADMSC-derived exosomes was comparable with healthy ADMSC-derived exosomes for treatment of the SS setting.

Clinical observational studies have clearly identified that SS frequently affected multiple organs [17], especially those preponderant in kidney and lung. Our previous studies have also shown that both kidney and lung organs are commonly organs vulnerable to damage in the SS setting [37]. A principal finding in the present study was that not only the kidneys but also the lungs were damaged by SS. Our experimental finding supported the previous clinical observational studies [17] that multiple organs were inevitable involved and damaged in settings of SS. Of particular importance was that apoptotic ADMSC-derived or healthy ADMSC-derived exosome therapy effectively protected the lung and kidney from SS-induced injury.

Study limitations

This study has limitations. First, we did not determine the optimal dosage of apoptotic ADMSC-derived exosomes and healthy ADMSC-derived exosomes for the treatment of SS.

Therefore, we do not know whether the former is superior to the later or vice versa for suppressing SS-induced organ damage and improving the prognostic outcome. Second, despite extensive work in the present study, the exact underlying mechanism of SS in multi-organ damage was still not fully identified. Third, although the short-term outcome (i.e., the study period was only five days) were attractive and promising, the long-term outcome remains uncertain.

In conclusion, the results of the present study showed that not only localized but also systemically inflammatory reactions were elicited by SS. Apoptotic ADMSC-derived exosomes might be inferior to healthy ADMSC-derived exosomes for reducing the multi-organ damage and mortality rate in rodents after SS.

Acknowledgements

This work was supported by research grants from Chang Gung Memorial Hospital, Chang Gung University (Grant no. CMRPG8F0541 and CMRPG8F0542).

Disclosure of conflict of interest

None.

Address correspondence to: Hong-Hwa Chen, Division of Cardiology, Department of Internal Medicine, Kaohsiung Chang Gung Memorial Hospital and Chang Gung University College of Medicine, 123 Dapi Road, Niaosung Dist., Kaohsiung 83301, Taiwan, China. Tel: +886-7-7317123; Fax: +886-7-7322402; E-mail: ma2561@adm.cgmh.org.tw

References

[1] Angus DC, Linde-Zwirble WT, Lidicker J, Clermont G, Carcillo J and Pinsky MR. Epidemiology of severe sepsis in the United States: analysis of incidence, outcome, and associated costs of care. Crit Care Med 2001; 29: 1303-1310.

[2] Brun-Buisson C, Meshaka P, Pinton P, Vallet B; EPISEPSIS Study Group. EPISEPSIS: a reappraisal of the epidemiology and outcome of severe sepsis in French intensive care units. Intensive Care Med 2004; 30: 580-588.

[3] Brun-Buisson C, Roudot-Thoraval F, Girou E, Grenier-Sennelier C and Durand-Zaleski I. The costs of septic syndromes in the intensive care unit and influence of hospital-acquired sepsis. Intensive Care Med 2003; 29: 1464-1471.

[4] Dellinger RP, Levy MM, Carlet JM, Bion J, Parker MM, Jaeschke R, Reinhart K, Angus DC, Brun-Buisson C, Beale R, Calandra T, Dhainaut JF, Gerlach H, Harvey M, Marini JJ, Marshall J, Ranieri M, Ramsay G, Sevransky J, Thompson BT, Townsend S, Vender JS, Zimmerman JL, Vincent JL; International Surviving Sepsis Campaign Guidelines Committee; American Association of Critical-Care Nurses; American College of Chest Physicians; American College of Emergency Physicians; Canadian Critical Care Society; European Society of Clinical Microbiology and Infectious Diseases; European Society of Intensive Care Medicine; European Respiratory Society; International Sepsis Forum; Japanese Association for Acute Medicine; Japanese Society of Intensive Care Medicine; Society of Critical Care Medicine; Society of Hospital Medicine; Surgical Infection Society; World Federation of Societies of Intensive and Critical Care Medicine. Surviving sepsis campaign: international guidelines for management of severe sepsis and septic shock: 2008. Crit Care Med 2008; 36: 296-327.

[5] Dellinger RP, Levy MM, Rhodes A, Annane D, Gerlach H, Opal SM, Sevransky JE, Sprung CL, Douglas IS, Jaeschke R, Osborn TM, Nunnally ME, Townsend SR, Reinhart K, Kleinpell RM, Angus DC, Deutschman CS, Machado FR, Rubenfeld GD, Webb S, Beale RJ, Vincent JL, Moreno R; Surviving Sepsis Campaign Guidelines Committee including The Pediatric Subgroup. Surviving sepsis campaign: international guidelines for management of severe sepsis and septic shock, 2012. Intensive Care Med 2013; 39: 165-228.

[6] Seymour CW, Liu VX, Iwashyna TJ, Brunkhorst FM, Rea TD, Scherag A, Rubenfeld G, Kahn JM, Shankar-Hari M, Singer M, Deutschman CS, Escobar GJ and Angus DC. Assessment of clinical criteria for sepsis: for the third international consensus definitions for sepsis and septic shock (sepsis-3). JAMA 2016; 315: 762-774.

[7] Singer M, Deutschman CS, Seymour CW, Shankar-Hari M, Annane D, Bauer M, Bellomo R, Bernard GR, Chiche JD, Coopersmith CM, Hotchkiss RS, Levy MM, Marshall JC, Martin GS, Opal SM, Rubenfeld GD, van der Poll T, Vincent JL and Angus DC. The third international consensus definitions for sepsis and septic shock (sepsis-3). JAMA 2016; 315: 801-810.

[8] Cronshaw HL, Daniels R, Bleetman A, Joynes E and Sheils M. Impact of the surviving sepsis campaign on the recognition and management of severe sepsis in the emergency department: are we failing? Emerg Med J 2011; 28: 670-675.

[9] Hotchkiss RS and Karl IE. The pathophysiology and treatment of sepsis. N Engl J Med 2003; 348: 138-150.
[10] Hein F, Massin F, Cravoisy-Popovic A, Barraud D, Levy B, Bollaert PE and Gibot S. The relationship between CD4+CD25+CD127- regulatory T cells and inflammatory response and outcome during shock states. Crit Care 2010; 14: R19.
[11] Taylor AL and Llewelyn MJ. Superantigen-induced proliferation of human CD4+CD25- T cells is followed by a switch to a functional regulatory phenotype. J Immunol 2010; 185: 6591-6598.
[12] Venet F, Chung CS, Monneret G, Huang X, Horner B, Garber M and Ayala A. Regulatory T cell populations in sepsis and trauma. J Leukoc Biol 2008; 83: 523-535.
[13] Venet F, Chung CS, Kherouf H, Geeraert A, Malcus C, Poitevin F, Bohe J, Lepape A, Ayala A and Monneret G. Increased circulating regulatory T cells (CD4(+)CD25(+)CD127(-)) contribute to lymphocyte anergy in septic shock patients. Intensive Care Med 2009; 35: 678-686.
[14] Hartemink KJ and Groeneveld AB. The hemodynamics of human septic shock relate to circulating innate immunity factors. Immunol Invest 2010; 39: 849-862.
[15] Monserrat J, de Pablo R, Reyes E, Diaz D, Barcenilla H, Zapata MR, De la Hera A, Prieto A and Alvarez-Mon M. Clinical relevance of the severe abnormalities of the T cell compartment in septic shock patients. Crit Care 2009; 13: R26.
[16] Maury E, Blanchard HS, Chauvin P, Guglielminotti J, Alzieu M, Guidet B and Offenstadt G. Circulating endotoxin and antiendotoxin antibodies during severe sepsis and septic shock. J Crit Care 2003; 18: 115-120.
[17] Fry DE. Sepsis, systemic inflammatory response, and multiple organ dysfunction: the mystery continues. Am Surg 2012; 78: 1-8.
[18] Akyurekli C, Le Y, Richardson RB, Fergusson D, Tay J and Allan DS. A systematic review of preclinical studies on the therapeutic potential of mesenchymal stromal cell-derived microvesicles. Stem Cell Rev 2015; 11: 150-160.
[19] Burger D, Vinas JL, Akbari S, Dehak H, Knoll W, Gutsol A, Carter A, Touyz RM, Allan DS and Burns KD. Human endothelial colony-forming cells protect against acute kidney injury: role of exosomes. Am J Pathol 2015; 185: 2309-2323.
[20] Rossol-Allison J and Ward CJ. Exosomes to the rescue. J Am Soc Nephrol 2015; 26: 2303-2304.
[21] Chen HH, Lai PF, Lan YF, Cheng CF, Zhong WB, Lin YF, Chen TW and Lin H. Exosomal ATF3 RNA attenuates pro-inflammatory gene MCP-1 transcription in renal ischemia-reperfusion. J Cell Physiol 2014; 229: 1202-1211.
[22] Chen KH, Chen CH, Wallace CG, Yuen CM, Kao GS, Chen YL, Shao PL, Chen YL, Chai HT, Lin KC, Liu CF, Chang HW, Lee MS and Yip HK. Intravenous administration of xenogenic adipose-derived mesenchymal stem cells (ADMSC) and ADMSC-derived exosomes markedly reduced brain infarct volume and preserved neurological function in rat after acute ischemic stroke. Oncotarget 2016; 7: 74537-74556.
[23] Fleig SV and Humphreys BD. Rationale of mesenchymal stem cell therapy in kidney injury. Nephron Clin Pract 2014; 127: 75-80.
[24] Ko SF, Yip HK, Zhen YY, Lee CC, Lee CC, Huang CC, Ng SH and Lin JW. Adipose-derived mesenchymal stem cell exosomes suppress hepatocellular carcinoma growth in a rat model: apparent diffusion coefficient, natural killer T-cell responses, and histopathological features. Stem Cells Int 2015; 2015: 853506.
[25] Zhou Y, Xu H, Xu W, Wang B, Wu H, Tao Y, Zhang B, Wang M, Mao F, Yan Y, Gao S, Gu H, Zhu W and Qian H. Exosomes released by human umbilical cord mesenchymal stem cells protect against cisplatin-induced renal oxidative stress and apoptosis in vivo and in vitro. Stem Cell Res Ther 2013; 4: 34.
[26] Zou X, Zhang G, Cheng Z, Yin D, Du T, Ju G, Miao S, Liu G, Lu M and Zhu Y. Microvesicles derived from human Wharton's Jelly mesenchymal stromal cells ameliorate renal ischemia-reperfusion injury in rats by suppressing CX3CL1. Stem Cell Res Ther 2014; 5: 40.
[27] Le Blanc K, Tammik L, Sundberg B, Haynesworth SE and Ringden O. Mesenchymal stem cells inhibit and stimulate mixed lymphocyte cultures and mitogenic responses independently of the major histocompatibility complex. Scand J Immunol 2003; 57: 11-20.
[28] Sun CK, Yen CH, Lin YC, Tsai TH, Chang LT, Kao YH, Chua S, Fu M, Ko SF, Leu S and Yip HK. Autologous transplantation of adipose-derived mesenchymal stem cells markedly reduced acute ischemia-reperfusion lung injury in a rodent model. J Transl Med 2011; 9: 118.
[29] Chen YT, Sun CK, Lin YC, Chang LT, Chen YL, Tsai TH, Chung SY, Chua S, Kao YH, Yen CH, Shao PL, Chang KC, Leu S and Yip HK. Adipose-derived mesenchymal stem cell protects kidneys against ischemia-reperfusion injury through suppressing oxidative stress and inflammatory reaction. J Transl Med 2011; 9: 51.
[30] Chang CL, Leu S, Sung HC, Zhen YY, Cho CL, Chen A, Tsai TH, Chung SY, Chai HT, Sun CK, Yen CH and Yip HK. Impact of apoptotic adipose-derived mesenchymal stem cells on attenuating organ damage and reducing mortal-

ity in rat sepsis syndrome induced by cecal puncture and ligation. J Transl Med 2012; 10: 244.

[31] Chen HH, Lin KC, Wallace CG, Chen YT, Yang CC, Leu S, Chen YC, Sun CK, Tsai TH, Chen YL, Chung SY, Chang CL and Yip HK. Additional benefit of combined therapy with melatonin and apoptotic adipose-derived mesenchymal stem cell against sepsis-induced kidney injury. J Pineal Res 2014; 57: 16-32.

[32] Yip HK, Chang YC, Wallace CG, Chang LT, Tsai TH, Chen YL, Chang HW, Leu S, Zhen YY, Tsai CY, Yeh KH, Sun CK and Yen CH. Melatonin treatment improves adipose-derived mesenchymal stem cell therapy for acute lung ischemia-reperfusion injury. J Pineal Res 2013; 54: 207-221.

[33] Zhu W, Chen J, Cong X, Hu S and Chen X. Hypoxia and serum deprivation-induced apoptosis in mesenchymal stem cells. Stem Cells 2006; 24: 416-425.

[34] Sun CK, Lee FY, Kao YH, Chiang HJ, Sung PH, Tsai TH, Lin YC, Leu S, Wu YC, Lu HI, Chen YL, Chung SY, Su HL and Yip HK. Systemic combined melatonin-mitochondria treatment improves acute respiratory distress syndrome in the rat. J Pineal Res 2015; 58: 137-150.

[35] Lin KC, Yip HK, Shao PL, Wu SC, Chen KH, Chen YT, Yang CC, Sun CK, Kao GS, Chen SY, Chai HT, Chang CL, Chen CH and Lee MS. Combination of adipose-derived mesenchymal stem cells (ADMSC) and ADMSC-derived exosomes for protecting kidney from acute ischemia-reperfusion injury. Int J Cardiol 2016; 216: 173-185.

[36] Sung PH, Chiang HJ, Wallace CG, Yang CC, Chen YT, Chen KH, Chen CH, Shao PL, Chen YL, Chua S, Chai HT, Chen YL, Huang TH, Yip HK and Lee MS. Exendin-4-assisted adipose derived mesenchymal stem cell therapy protects renal function against co-existing acute kidney ischemia-reperfusion injury and severe sepsis syndrome in rat. Am J Transl Res 2017; 9: 3167-3183.

[37] Sung PH, Chang CL, Tsai TH, Chang LT, Leu S, Chen YL, Yang CC, Chua S, Yeh KH, Chai HT, Chang HW, Chen HH and Yip HK. Apoptotic adipose-derived mesenchymal stem cell therapy protects against lung and kidney injury in sepsis syndrome caused by cecal ligation puncture in rats. Stem Cell Res Ther 2013; 4: 155.